Supporting information

Achieving ultra-dispersed 1T-Co-MoS_2@HMCS via space-confined engineering for highly efficient hydrogen evolution in universal pH

Changle Yue[a], Yan Zhou[b], Yang Liu[a], Chao Feng[a], Wenjing Bao[a], Fengyue Sun[a], Yongxiao Tuo[b], Yuan Pan[a], Yunqi Liu[a], Yukun Lu[a,*]

[a] *State Key Laboratory of Heavy Oil Processing, College of Chemistry and Chemical Engineering, China University of Petroleum (East China), Qingdao 266580, PR China*

[b] *School of Materials Science and Engineering, China University of Petroleum (East China), Qingdao 266580, PR China*

Corresponding authors:

E-*mail addresses*: lyk@upc.edu.cn (Yukun Lu),

Table of contents

Experimental

1. Chemicals and reagents

$(NH_4)_6Mo_7O_{24}·4H_2O$ (99%), $C_{12}H_{30}Br_2N_2$ (hexamethonium bromide, HMB, 99%), $C_6H_6O_2$ (resorcinol, 99%) and $C_{12}H_{28}O_4Si$ (tetrapropoxysilane, TPOS, 97%) were purchased from Sangon Biotech (Shanghai, China). $Co(CH_3COO)_2·4H_2O$ (cobalt acetate tetrahydrate, AR, 99.5%), activated charcoal (200 mesh powder), CH_2O (formaldehyde solution, AR, 37% wt in water), HF (hydrofluoric acid, AR, 40.0%), C_2H_6O (ethanol, AR, ≥99.7%), KOH (potassium hydroxide, 95%), CH_4N_2S (thiourea, AR, 99%), MoO_3 (molybdenum oxide, AR, 99.5%) and $NH_3·H_2O$ (ammonium hydroxide solution, AR, 25 ~ 28%) were purchased from Macklin Biochem (Shanghai, China). H_2O_2 solution (Hydrogen peroxide solution, 30% wt in water) was purchased from Aladdin Biochem (Shanghai, China). H_2SO_4 (sulfuric acid, AR, 95 ~ 98%) and Nafion117 solution (~ 5% in a mixture of lower aliphatic alcohols and water) were purchased from Sinopharm Chem (Shanghai, China). 20% Pt/C catalysts was purchased from Alfa Aesar (Tianjin, China). All aqueous solutions were prepared with water from a Milli-Q Pore water system (18.2 MΩ).

2. Experimental section

All the chemicals used in this study were purchased without any further purification.

2.1 Preparation of HMCS

HMCS was synthesized according to the published procedure. [1] 6.00 mL $NH_3·H_2O$ was added to 160 mL aqueous solution of ethanol ($V_{ethanol}$: V_{water} = 7: 1) to obtain an alkaline environment. After sufficient magnetically stirring, 7.00 mL TPOS (24.2 mmol) was added slowly to the solution and stirring for 30 min. 1.12 mL CH_2O (13.8 mmol) solution and 0.800 g $C_6H_6O_2$ (7.27 mmol) dissolved in 4.00 mL ethanol by ultrasonic were slowly dropped into the above solution. After stirring for 24 h at room temperature, the light yellow SiO_2 precipitates were separated from the creamy white solution by centrifugation and dried at 60 ℃. The SiO_2 powder was then carbonized at 900 ℃ for 4 h under N_2 (99.999%) atmosphere with a heating rate of 5 ℃/min, followed

by natural cooling to produce black SiO_2@C spheres. The black HMCS powder could be obtained by SiO_2@C spheres stirred in a 13% wt. HF solution for 2 days.

2.2 Preparation of $(NH_4)_6[Co_2Mo_{10}H_4O_{38}]\cdot 4H_2O$ (Co_2Mo_{10})

Ammonium salt of decamolybdodicobaltate Co_2Mo_{10} was synthesized according to the published procedure. [2] 15.0 g (12.1 mmol) $(NH_4)_6Mo_7O_{24}\cdot 4H_2O$ and 3.10 g (12.4 mmol) $Co(CH_3COO)_2\cdot 4H_2O$ were dissolved in 125 mL water, then 3.00 g active charcoal and 20.0 mL peroxide solution (18%) were added to the solution. After boiling the black solution for 1 h, the active charcoal was separated by filtration. Dark-green Co_2Mo_{10} crystals were obtained by slow evaporation of the solvent at room temperature.

2.3 Synthesis of $(Co_2Mo_{10})(HM)_3$@HMCS

Co_2Mo_{10} was used as the Co source and Mo source. 0.248 g (0.133 mmol) Co_2Mo_{10} and 0.144 g (0.399 mmol) hexamethonium (HM) bromide were dissolved in 20.0 mL deionized water. Then, 30.0 mg HMCS was added to the clear green solution and stirred at room temperature for 12 h to obtain $(Co_2Mo_{10})(HM)_3$@HMCS. The black $(Co_2Mo_{10})(HM)_3$@HMCS precipitates were separated by centrifugation, washed by deionized water several times and dried at 60 ℃ for 24 h.

2.4 Synthesis of 1T-Co-MoS_2@HMCS

1T-Co-MoS_2@HMCS was obtained through calcining $(Co_2Mo_{10})(HM)_3$@HMCS under 10% vol. H_2S/H_2 at 400 ℃ for 4 h with the heating rate of 5 °C/min.

2.5 Synthesis of Co-MoS_2@HMCS

Co-MoS_2@HMCS was obtained without HM compared with 1T-Co-MoS_2@HMCS. 0.248 g (0.133 mmol) Co_2Mo_{10} was dissolved in 20 mL deionized water for 30 min. Then, 30.0 mg HMCS was added to the above solution and stirred for 12 h. The black as-synthesized product was separated by centrifugation, washed by deionized water several times and then dried at 60 ℃ for 24 h. Then the prepared sample was further calcined under 10% vol. H_2S/H_2 at 400 ℃ for 4 h with the heating rate of 5 °C/min, followed by natural cooling to produce Co-MoS_2@HMCS powder.

2.6 Synthesis of Co-MoS_2

Co-MoS_2 was prepared by calcining the Co_2Mo_{10} at 400 ℃ for 4 h with the heating

rate of 5 °C/min under 10% vol. H_2S/H_2 atmosphere.

2.7 Synthesis of MoS_2@HMCS and CoS@HMCS

0.282 g (0.228 mmol) $(NH_4)_6Mo_7O_{24}\cdot 4H_2O$ or 0.398 g (1.60 mmol) $Co(CH_3COO)_2\cdot 4H_2O$ was dissolved in 20.0 mL deionized water containing 0.144 g (0.399 mmol) hexamethonium (HM) bromide for 30 min. Then 30.0 mg HMCS was added to the above solution and stirred for 12 h. The as-synthesized product was separated by centrifugation and washed by deionized water several times and then dried at 60 ℃ for 24 h. Then the prepared sample was further calcined under 10% vol. H_2S/H_2 at 400 ℃ for 4 h with the heating rate of 5 °C/min, followed by natural cooling to produce MoS_2@HMCS or CoS@HMCS powder.

2.8 Synthesis of 2H-MoS_2

Hydrothermal synthesis in a sealed autoclave system was used for preparation of 2H-MoS_2. First, 1.44 g (10 mmol) MoO_3 and 3.04 g (40 mmol) CH_4N_2S were dispersed in 70 mL deionized water under stirring to form a homogeneous solution. Then, the above solution was transferred into a 100 ml Teflon-lined stainless steel autoclave, kept at 220 ℃ for 12 h. The final product was purified with deionized water for several times and dried at 60 ℃.

2.9 Structural characterizations

X-ray powder diffraction (XRD) patterns of the products were tested with an X-ray diffractometer (BRUKER D8 ADVANCE) by Cu Kα radiation (λ = 1.5418 Å, 40 kV, 40 mA) at room temperature. Scanning electron microscope (SEM) images of the products were captured by a field-emission SEM (JMS-7900F). High-resolution transmission electron microscopy (HRTEM) , energy dispersive X-ray spectroscopy (EDX) images and annular dark-field STEM of the products were obtained by HRTEM (JEM-2100F). The Fourier transform infrared spectroscopy (FT-IR) was recorded on a VERTEX 80 V FT-IR spectrometer. The chemical states of the sample were determined by X-ray photoelectron spectroscopy (XPS) with a Thermo VG ESCALAB250XI surface analysis system. N_2 adsorption-desorption isotherms were obtained using a Quantachrome Autosorb-1-MP analyzer at 77 K and the specific surface area was calculated automatically using a multipoint Brunauer-Emmett-Teller (BET) model.

Raman spectra of the catalysts were recorded on a Senterra laser Raman spectrometer (λ = 532 nm) equipped with an optical microscope in confocal mode.

2.10 Electrochemical characterizations

All of the electrochemical performance tests in 1.0 M KOH and 0.5 M H_2SO_4 electrolyte media were performed on Gamry INTERFACE 1000 E, USA, using an Saturated calomel electrode (SCE) electrode, a graphite rod, and as-prepared bimetal sulfide electrodes as the reference electrode, the counter electrode, and the working electrode, respectively. All polarization curves at 2 $mV \cdot s^{-1}$ were iR compensated. The linear sweep voltammetry (LSV) measurements were recorded with a scan rate of 2 $mV \cdot s^{-1}$. The cyclic voltammetry (CV) measurements were carried out with different sweep rates between 40 and 200 $mV \cdot s^{-1}$. The long-term stability tests were performed by CV tests at the scan rate of 100 $mV \cdot s^{-1}$. The electrochemical Impedance Spectroscopy (EIS) tests wemeasured by ac impedance spectroscopy in the frequency range of 10° to 1 Hz. According to the Nernst equation $E_{RHE} = E_{SCE} + 0.059pH + 0.254$, where E_{RHE} is the potential vs a reversible hydrogen electrode, E_{SCE} is the potential vs an SCE electrode, and pH is the pH value of the electrolyte.

The surface of the glassy carbon electrode (GCE, 3 mm diameter) was polished with 0.3 μm alumina slurries, and sonicated with deionized water and ethanol. Then the electrode was dried at 25 ℃. To prepare the modified electrodes, 5.0 mg of the electrocatalyst was dispersed into 1.005 mL of Nafion solution [5.0 μL Nafion (5%) dissolved in 1.000 mL of ethanol] to give homogeneous suspension upon bath sonication. A drop 20.0 μL of the suspension was dropped onto GCE surface and the electrode was dried at 25 ℃.

2.11 Computational methods

Spin-polarized density functional theory (DFT) calculations were performed using Vienna ab initio simulation packages (VASP) and employed using the generalized gradient approximation (GGA) with Perdew-Burke-Ernzerhof (PBE) functional to describe the exchange and correlation energy in all calculations.[3] The projector-augmented wave (PAW) method was used to represent the interactions between valence electrons and ionic cores. The plane wave cutoff energy was fixed at 400 eV. To model

the MoS_2-Co, a 1T-MoS_2 slab with exposed [001] surface was used, resulting in the model with the lowest lattice mismatch for following calculation. The supercell consists of 3 × 3 unit cells for MoS_2 slab, with a 10 Å vacuum region to simulate the adsorption. The all layers together with the adsorbates were fully relax in all dimensions until the maximum force on a single atom was smaller than 0.03 $eV \cdot Å^{-1}$ and the convergence of energy and forces were set to 1×10^{-4} Ha. The Brillouin zone was sampled by the Monkhorst-Pack method with an 8 × 8 × 1 k-point mesh.

For hydrogen evolution reaction (HER) in acid environment, the reaction Gibbs free energy (ΔG_H^*) can be calculated as follows: [4, 5]

$$\Delta G_H^* = \Delta E_H + \Delta E_{ZPE} - T\Delta S_H$$

where ΔE_H, ΔE_{ZPE}, and ΔS_H are the adsorption energy of hydrogen, the zero-point energy difference and the entropy difference. In standard conditions, $\Delta E_{ZPE} - T\Delta S_H$ is about 0.24 eV, hence (ΔG_H^*) can be calculated by ΔE_H+0.24.

The (OER) in alkali environment follows three elementary steps. The free energies of the intermediates at 298.15 K were obtained by:

$$\Delta G_H = \Delta E + \Delta E_{ZPE} - T\Delta S_H + eU$$

Where $\Delta E_{ZPE,}$ ΔS and U are the zero-point energy changes, entropy changes and applied potentials. And ΔE is the binding energy of adsorption species HO*, O* and HOO*, with defined as follows:

$$\Delta E = E_{substrate+adsorbate} - E_{substrate} - E_{adsorbate}$$

References

[1] X.K. Wan, H.B. Wu, B.Y. Guan, D. Luan, X.W. Lou, Confining Sub-Nanometer Pt Clusters in Hollow Mesoporous Carbon Spheres for Boosting Hydrogen Evolution Activity, Adv. Mater., 32 (2020) 1901349.

[2] P.A. Nikulshin, A.V. Mozhaev, K.I. Maslakov, A.A. Pimerzin, V.M. Kogan, Genesis of HDT catalysts prepared with the use of Co2Mo10HPA and cobalt citrate: Study of their gas and liquid phase sulfidation, Appl. Catal. B: Environ., 158-159 (2014) 161-174.

[3] Z. Liu, C. Chen, J. Zhao, L. Yang, K. Sun, L. Zeng, Y. Pan, Y. Liu, C. Liu, Study

on the NO_2 production pathways and the role of NO_2 in fast selective catalytic reduction $DeNO_x$ at low-temperature over MnO_x/TiO_2 catalyst, Chemical Engineering Journal, 379 (2020) N.PAG-N.PAG.

[4] K. Sun, Y. Liu, Y. Pan, H. Zhu, J. Zhao, L. Zeng, Z. Liu, C. Liu, Targeted bottom-up synthesis of 1T-phase MoS_2 arrays with high electrocatalytic hydrogen evolution activity by simultaneous structure and morphology engineering, Nano Research, 11 (2018) 4368-4379.

[5] T. Xiong, X. Yuan, H. Wang, L. Jiang, Z. Wu, H. Wang, X. Cao, Integrating the (311) facet of MnO_2 and the fuctional groups of poly(m-phenylenediamine) in core–shell MnO_2@poly(m-phenylenediamine) adsorbent to remove Pb ions from water, J. Hazard. Mater., 389 (2020) 122154.

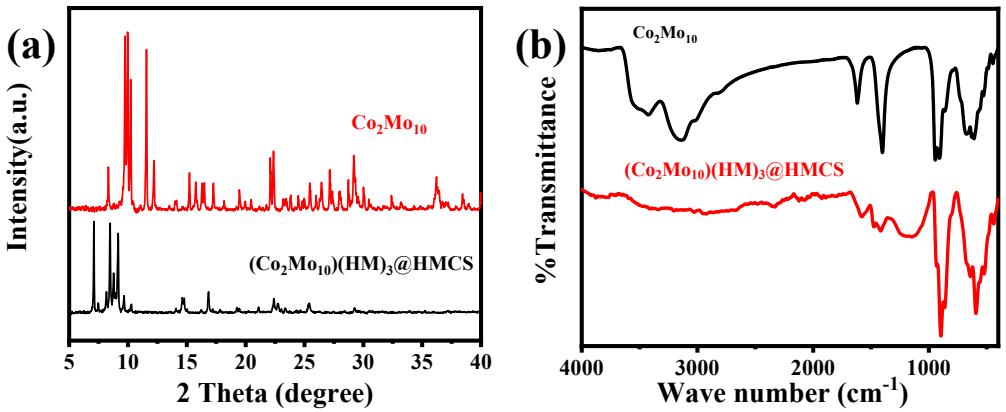

Fig. S1. (a) XRD patterns for Co_2Mo_{10} and $(Co_2Mo_{10})(HM)_3$@HMCS, (b) FT-IR

spectra for both Co_2Mo_{10} and $(Co_2Mo_{10})(HM)_3$@HMCS

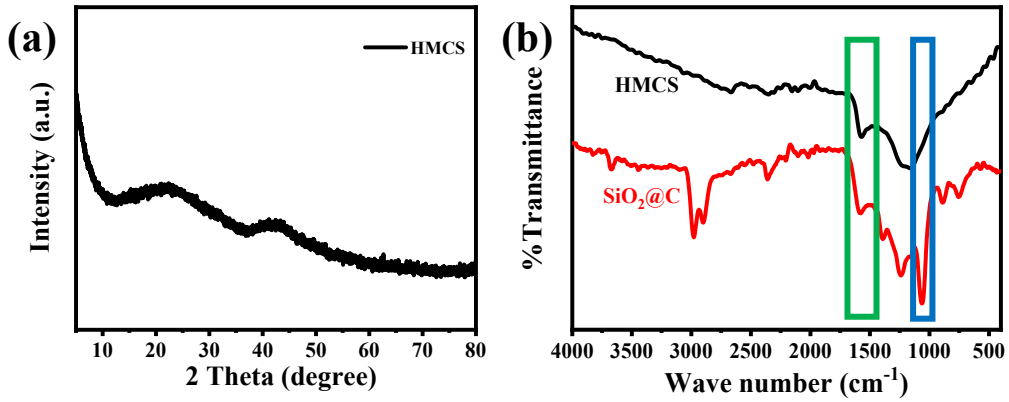

Fig. S2. (a) XRD patterns for HMCS, (b) IR spectra for both HMCS and SiO_2@C, the selected areas represent the vibrational bands for C=C and Si-O-C bonds.

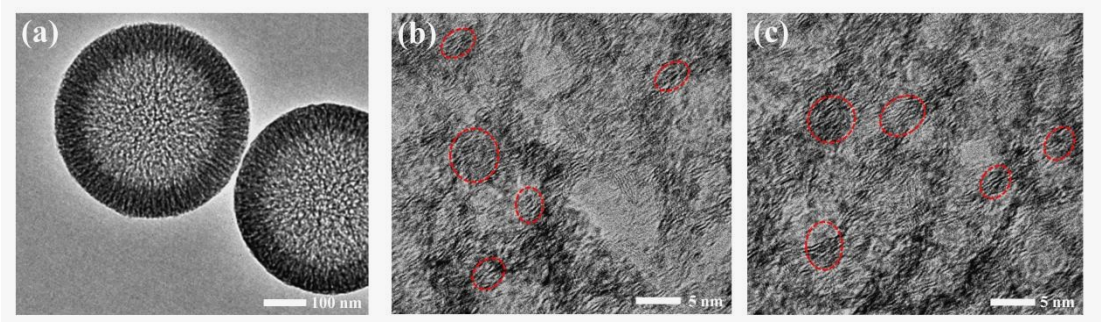

Fig. S3. TEM image (a) and HRTEM images (b and c) of Co-MoS_2@HMCS

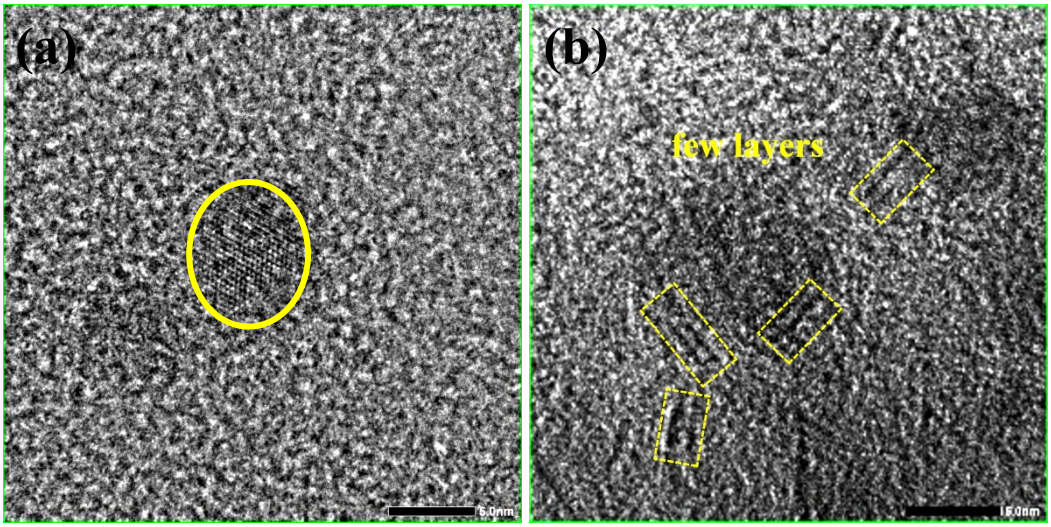

Fig. S4. HRTEM images of 1T-Co-MoS_2@HMCS.

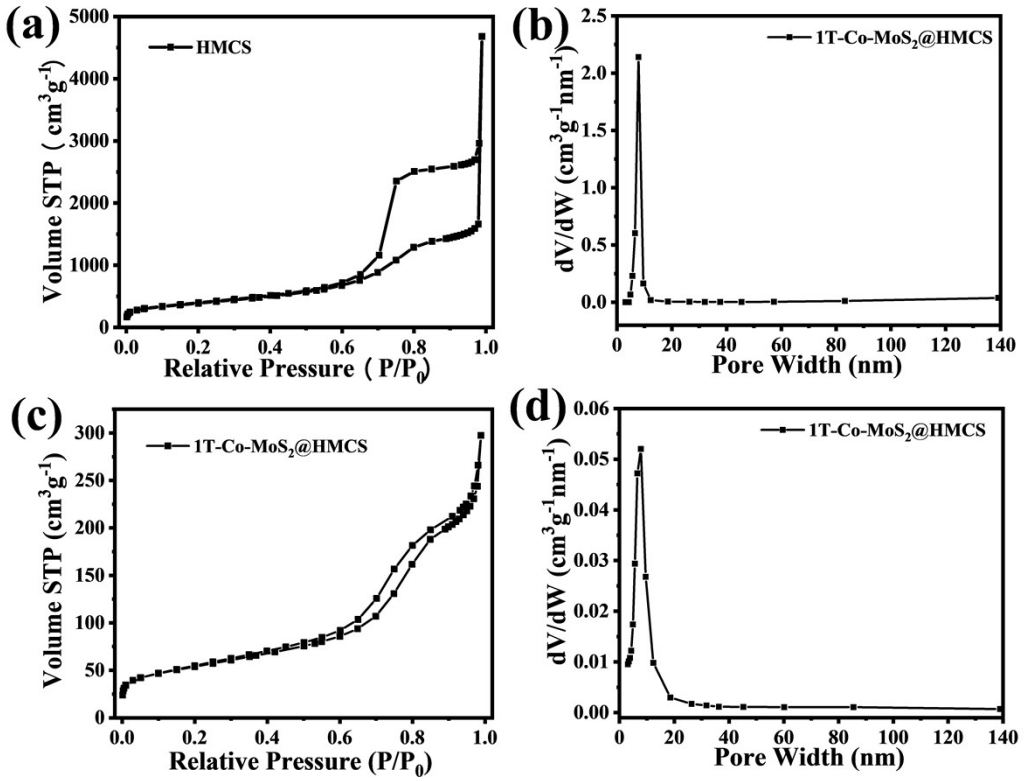

Fig. S5. (a) Nitrogen adsorption-desorption isotherms and (b) BJH pore distribution of HMCS, (c) Nitrogen adsorption-desorption isotherms and (d) BJH pore distribution of 1T-Co-MoS_2@HMCS.

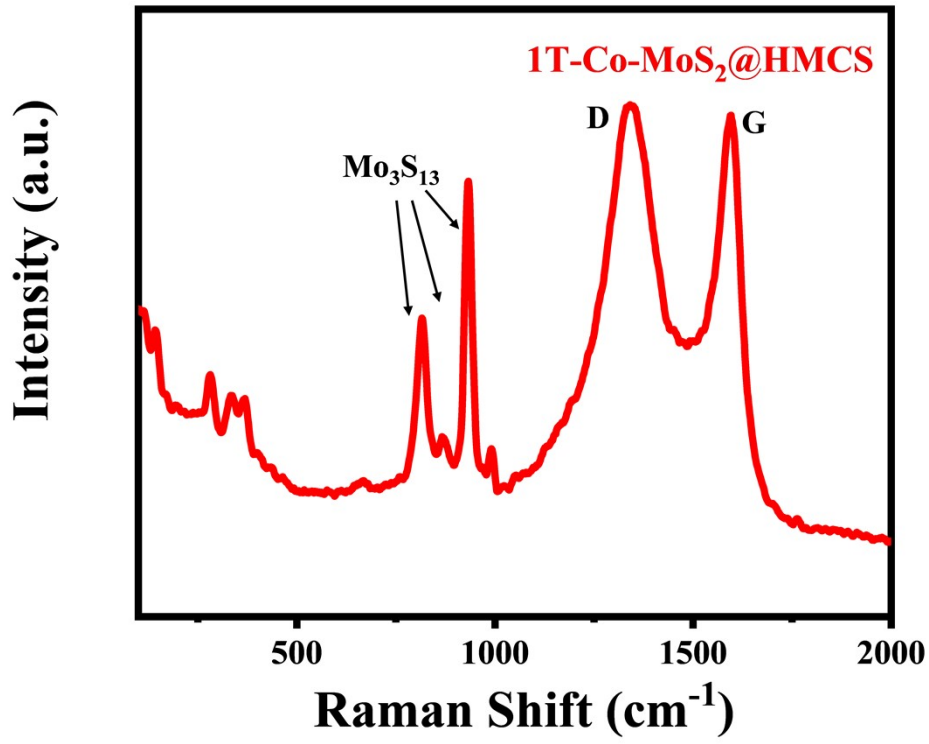

Fig. S6. Raman spectrum of 1T-Co-MoS_2@HMCS.

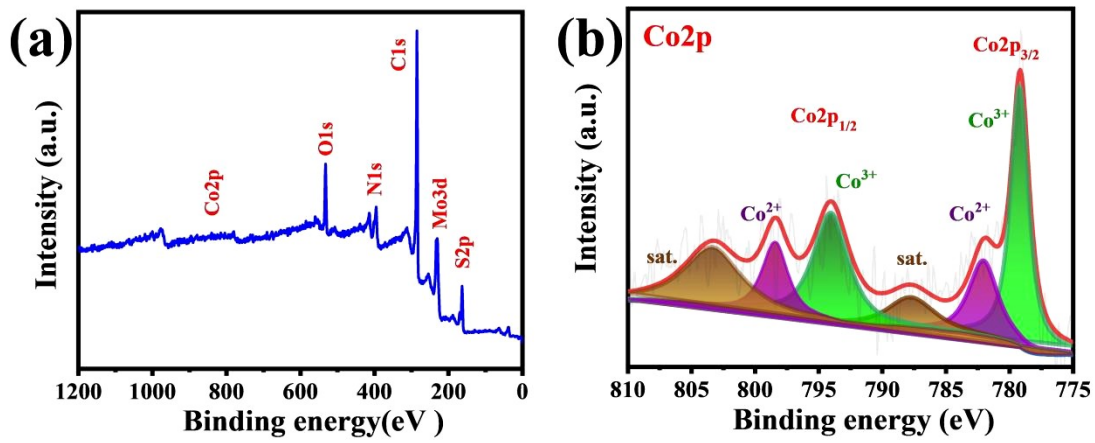

Fig. S7. (a) Full XPS spectrum and (b) high-resolution XPS spectra of Co 2p in 1T-Co-MoS_2@HMCS catalyst.

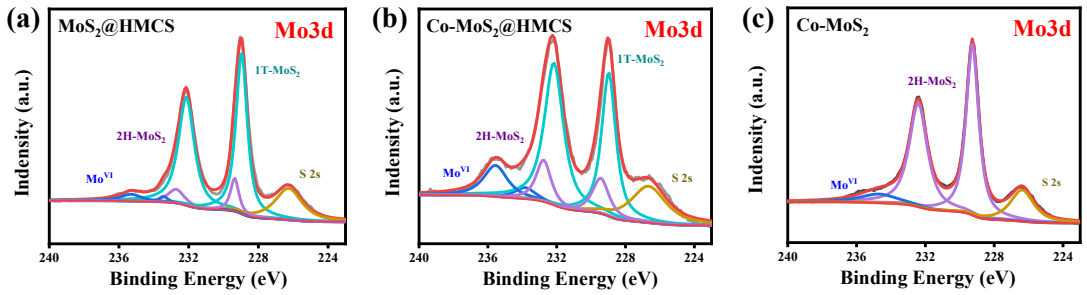

Fig. S8. High-resolution XPS spectra of Mo 3d in MoS_2@HMCS (a), Co-MoS_2@HMCS (b) and Co-MoS_2 (c).

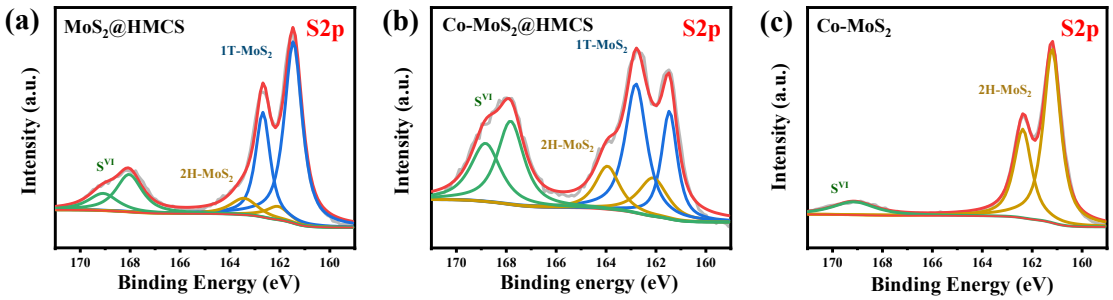

Fig. S9. High-resolution XPS spectra of S 2p in MoS_2@HMCS (a), Co-MoS_2@HMCS (b) and Co-MoS_2 (c).

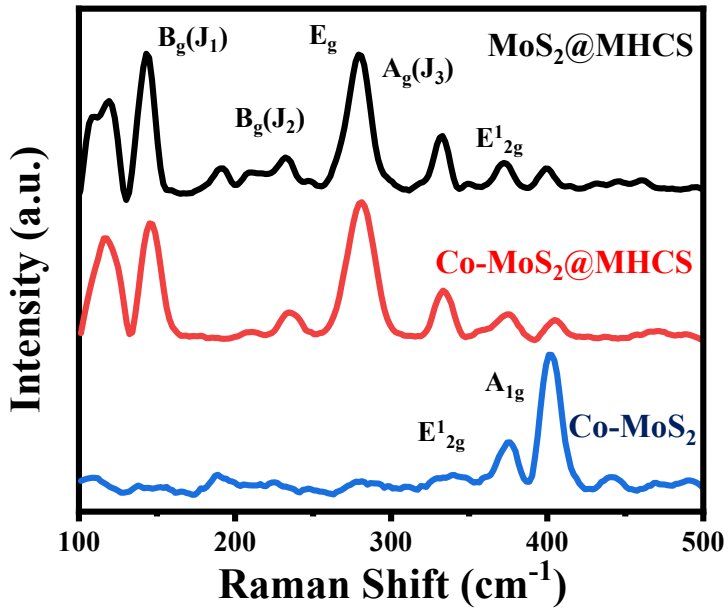

Fig. S10. Raman spectrum of MoS_2@HMCS, Co-MoS_2@HMCS and Co-MoS_2.

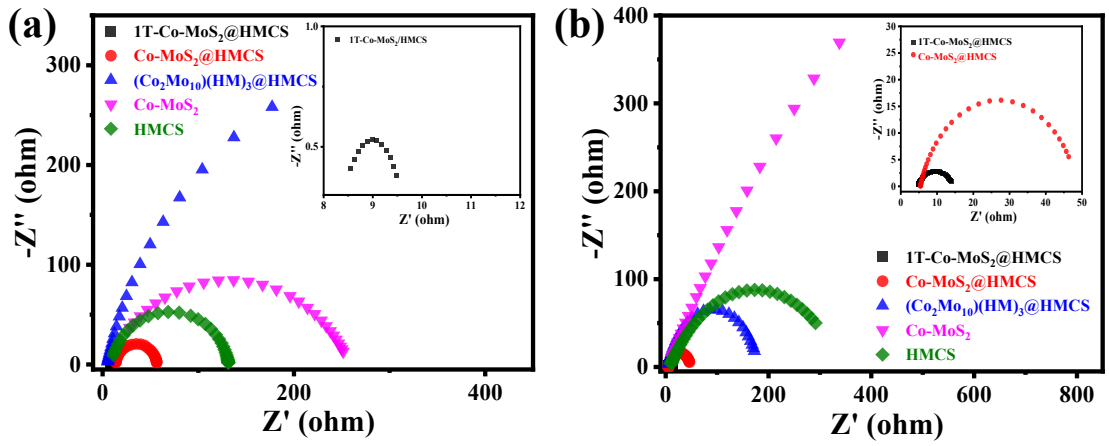

Fig. S11. Electrochemical impedance spectroscopy (EIS) of 1T-Co-MoS_2@HMCS, Co-MoS_2@HMCs, $(Co_2Mo_{10})(HM)_3$@HMCS, Co-MoS_2 and HMCS tested in (a) 1.0 M KOH and (b) 0.5 M H_2SO_4.

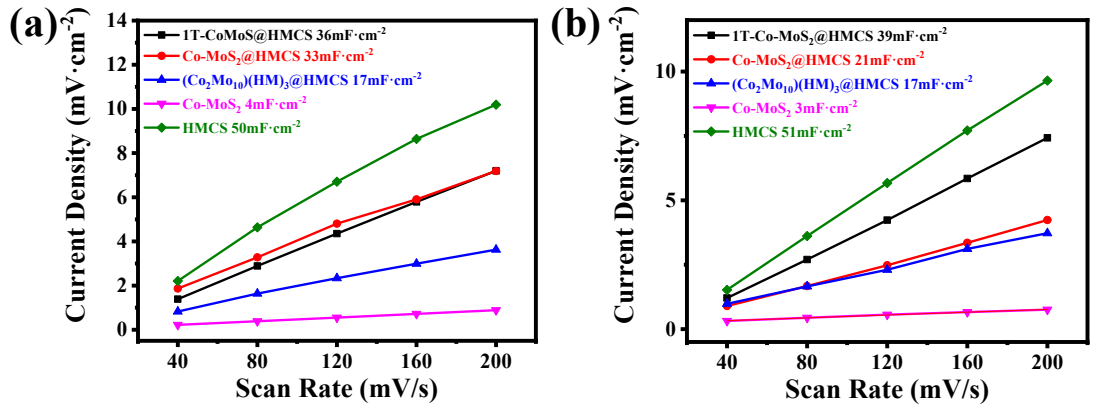

Fig. S12. Double-layer capacitance (C_{dl}) determined by plotting capacitive currents as function of scan rate in of alkaline (a) and acidic solutions (b).

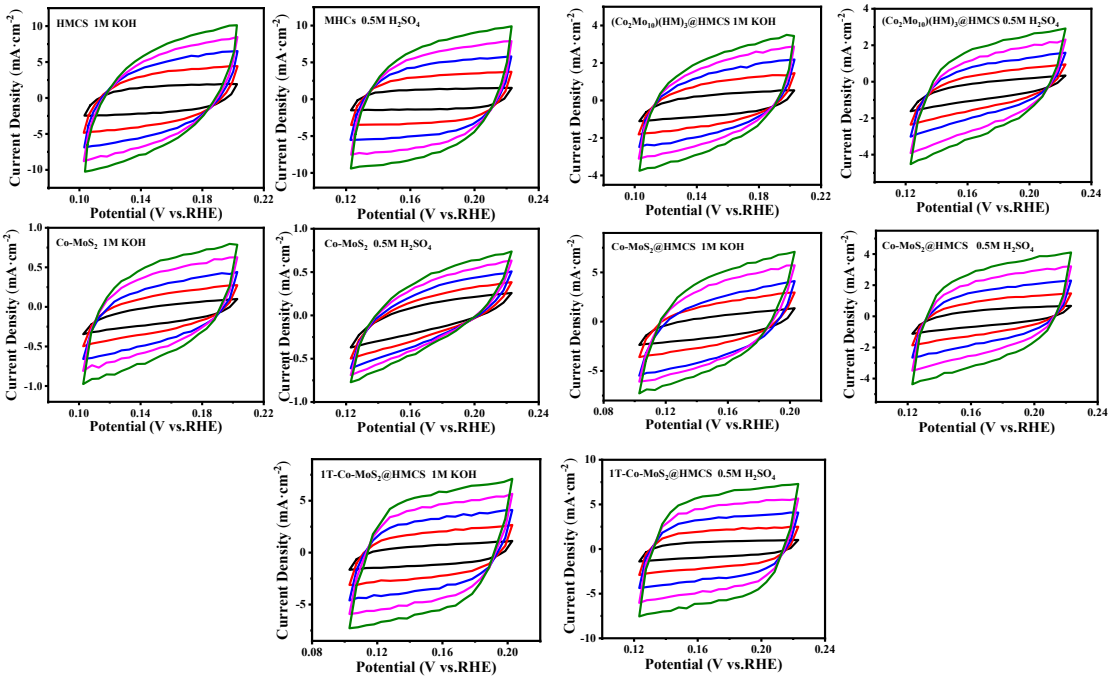

Fig. S13. CVs with different scan rates of different catalysts in 1.0 M KOH and 0.5 M H_2SO_4.

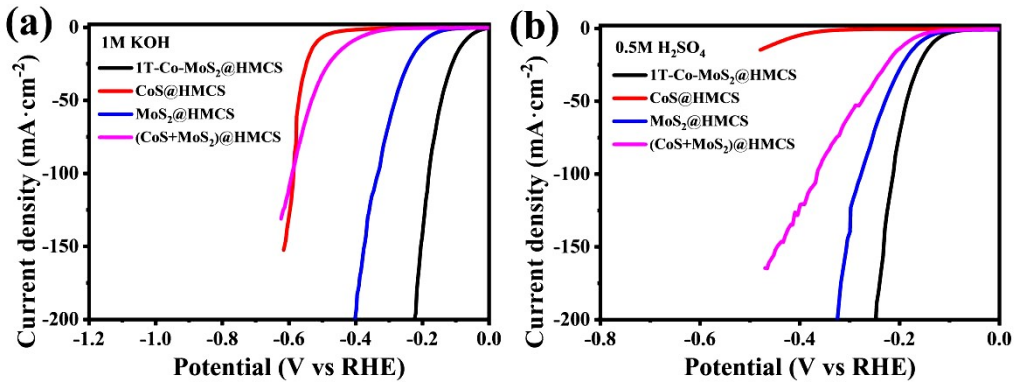

Fig. S14. HER polarization curves of different catalysts in 1.0 M KOH (a) and 0.5 M H_2SO_4.

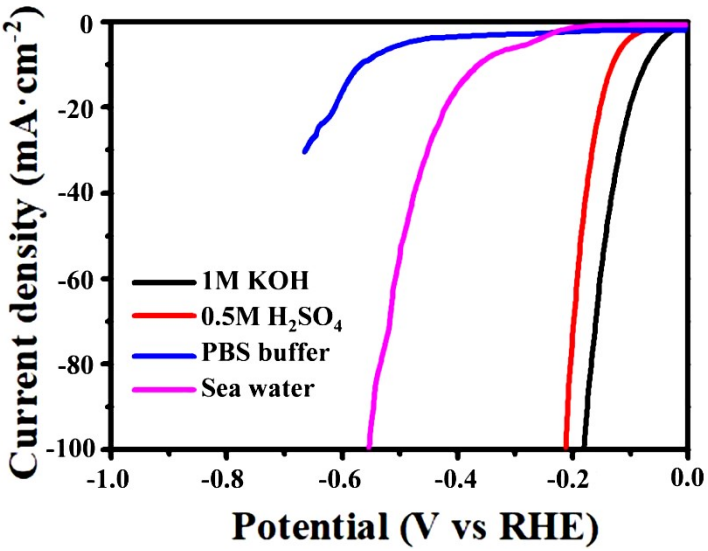

Fig. S15. HER polarization curves of 1T-Co-MoS_2@HMCS in different solutions.

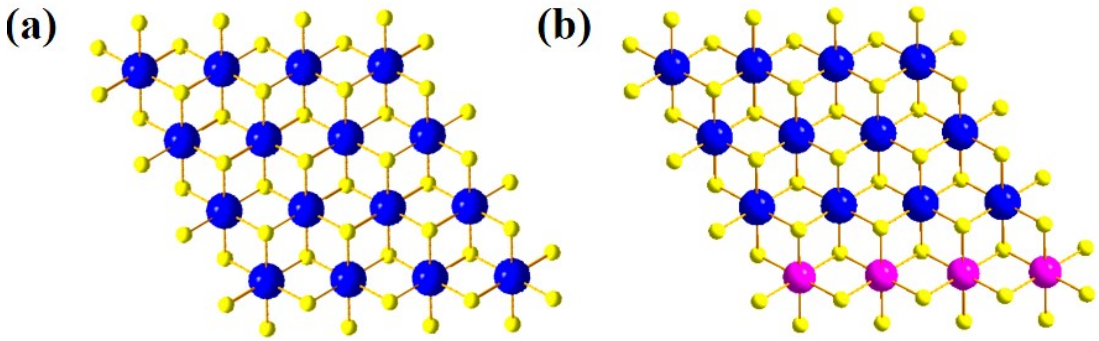

Fig. S16. The calculation model of 1T-MoS_2 and 1T-Co-MoS_2.

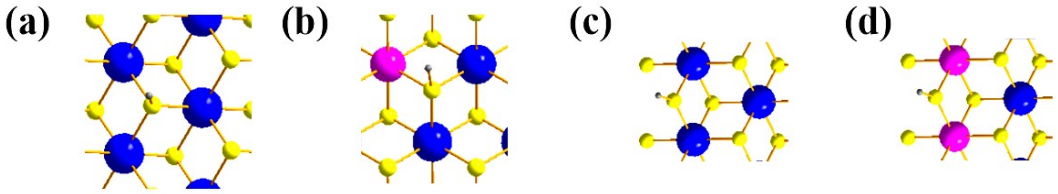

Fig. S17. The adsorption model of 1T-MoS_2 and 1T-Co-MoS_2 in acidic condition.

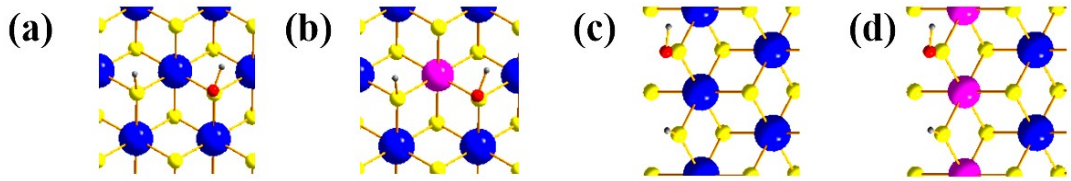

Fig. S18. The adsorption model of 1T-MoS_2 and 1T-Co-MoS_2 in alkaline condition.

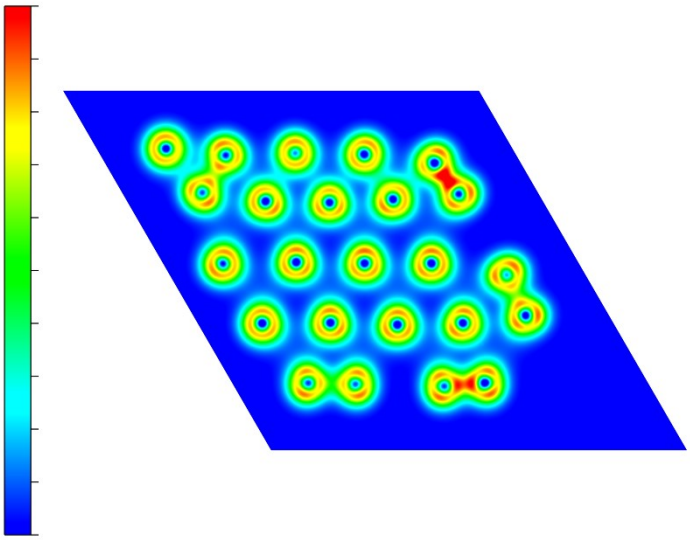

Fig. S19. Charge density diagram of 1T-Co-MoS_2.

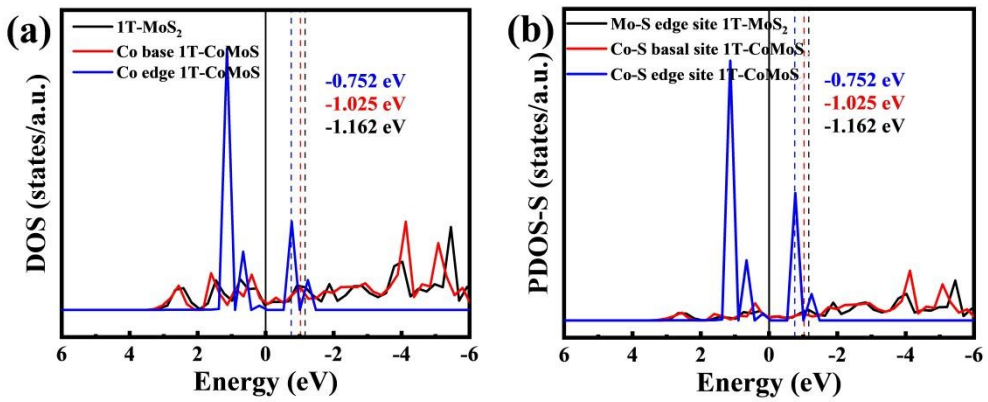

Fig. S20. Schematic of DOS and PDOS with different edges of 1T-MoS_2 and 1T-Co-MoS_2.

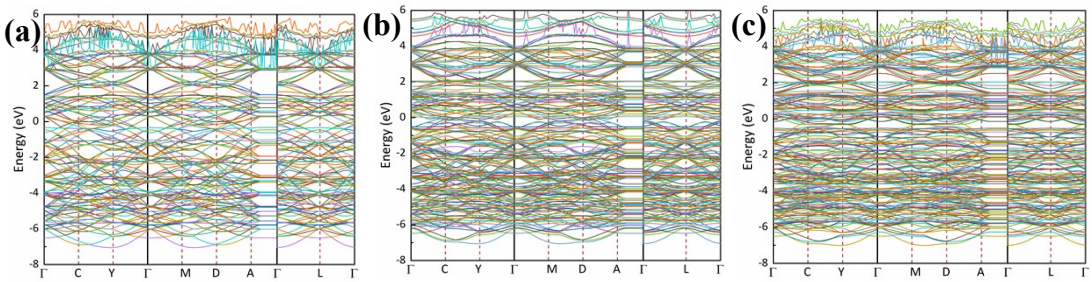

Fig. S21. Band structure of the effective model for the d bands of 1T-MoS_2, Co-S basal site and Co-S edge site of 1T-Co-MoS_2

Table S1. Comparison of HER Performance of 1T-Co-MoS_2@HMCS with Reported Electrocatalysts in 1.0 M KOH.

Electrocatalyst	Overpotential η (mV *vs*. RHE)	Tafel slops (mV dec^{-1})	References
1T-Co-MoS_2@HMCS	**η_{10} = 74**	**63**	**This work**
CN/CNL/MoS_2/CP	η_{10} = 106	117	*Chem. Eng. J*., **2021**, 412, 128556.
H-MoS_2/MoP	η_{10} = 97	57.8	*Small*, **2020**, 16, 2002482.
Mo_2S@NSCS	η_{10} = 206	94	*Appl. Catal. B: Environ*., **2020**, 263, 118352.
V- doped MoS_2	η_{10} = 206	89	*Appl. Catal. B: Environ.*, **2019**, 254, 432–442.
1T $MoS_2/Ni^{2+\delta}O_\delta(OH)_{2-\delta}$	η_{10} = 185	77	*Adv. Sci*., **2018**, 5, 1700644.
CoMoNiS-NF-31	η_{10} = 113	58	*J. Am. Chem. Soc.,* **2019**, 141, 26.
Co-Mo_2C@NCNT	η_{10} = 186	79	*ACS Sustainable Chem. Eng*., **2018**, 6, 9912−9920.
Mo_2C-GNR	η_{10} = 217	64	*ACS. Sustainable. Chem. Eng*., **2016**, 4, 6313−6321.
Mo_2N-Mo_2C/HGr	η_{10} = 154	68	*Adv. Mater*., **2018**, 30, 2, 1704156.
O-CoMoS	η_{10} = 97	70	*ACS Catal.,* **2018**, 8, 4612−4621.
1T-MoS_2/NiS_2	η_{10} = 116	72	*Angew. Chem. Int. Ed.,* **2019**, 58, 17621−17624.
$CoS_{1.097}/MoS_2$	η_{10} = 249	75	*ACS Appl. Energy Mater.,* **2019**, 2, 7504−7511.

Table S2. Comparison of HER performance of 1T-Co-MoS_2@HMCS with reported electrocatalysts in 0.5 M H_2SO_4.

Electrocatalyst	Overpotential η(mV)	Tafel slops (mV dec^{-1})	References
1T-Co-MoS_2@HMCS	**η_{10} = 132**	**78**	**This work**
1rGO-MoS_2	η_{10} = 197	230	*ACS Appl. Mater. Interfaces.*, **2020**, 12, 12629−12638.
Mo_2C/N-PC	η_{10} = 178	72	*J. Mater. Chem. A*, **2019**, 7, 4734-4743.
np-Mo_2C	η_{10} = 229	101	*Adv. Sci.*, **2017**, 1700601.
$CoS_{1.097}$/MoS_2	η_{10} = 228	59	*ACS Appl. Energy Mater.*, **2019**, 2, 7504−7511.
P-Mo_2C/Ti_3C_2@NC	η_{10} = 177	57.3	*ACS Sustainable Chem. Eng.*, **2020**, 8, 12990–12998.
Co−Mo−S/CC	η_{10} = 203	86	*Nanoscale*, **2018**, 10, 8404−8412.
3DHP-Mo_2C	η_{10} = 166	75	*J. Mater. Chem. A*, **2017**, 5, 20228–20238.
mPF-MoS_2	η_{10} = 210	-	*Nat. Commun.*, **2017**, 8, 14430.
np-Mo_2C	η_{10} = 229	101	*Adv. Sci.*, **2018**, 5, 1700601
Co/MoS_2	η_{10} = 156	58	*Nano Energy*, **2017**, 39, 409.
Ni-Fe-LDH-MoS_2-2	η_{10} = 180	82	*ACS Energy Lett.* **2018**, 3, 4, 952–960.
Ni/β-Mo_2C	η_{10} = 155	79	*Chem. Commun.*, **2018**, 54, 9901–9904